Original Research

Trefftz Method Applied to the Problem of Pumping Well Test Counter-Calculation

Yan Su, Lan Qing Huang, Ling Jun Yang, Hamed Benisi Ghadim*, Chuan Lin

Department of Water Resources and Harbor Engineering, College of Civil Engineering,
Fuzhou University, Fuzhou, China

Abstract

Nowadays, field pumping test is still the primary way to obtain accurate hydrogeological parameters, and high cost and low efficiency are still its main limitations. Therefore, it is still beneficial to study how to obtain hydrogeological parameters quickly and accurately. In this paper, the Trefftz method is applied in combination with the New Fictitious Time Integration Method（NFTIM）, to solve the groundwater reverse calculation problem with unknown partial boundary and effectively solve the discomfort in the reverse calculation problem. Based on the actual pumping test data of the ZK03 hole in the section V of Harbin Metro Line 3, the model was built. By verifying the analytical solution with the Thiem formula and comparing it with the observation well data, it is proved that the Trefftz inverse calculation method is more operable and has a high degree of accuracy (with average error of 9.94×10^{-10}). Concurrently, the hydrogeological parameters such as the influence radius, water head distribution, and depth drop curve of the pumping well are calculated to provide crucial for the design and construction of subway engineering.

Keywords: Trefftz method, counter-calculation, pumping well test, stabilizes flow, drop deep

Introduction

With the development of economy and society, the increase of deep foundation pit projects in the subway, underground commercial street, and other places inevitably brings about sand flow and pipe surge, which causes the collapse of the foundation pit other damage. Designers and builders pay the precipitation of the foundation pit more and more attention. Predicting and controlling the water table is often the key to ensuring the pit's safe construction, which involves the influence radius R of the submersible aquifer. At present, the methods for determining aquifer parameters usually include the Pumping test method, the Pressurized water test method, the Water injection test method, the Trace test method, etc [1]. However, such pumping tests generally require a large amount of exploration and test to provide data support, which significantly limits the conditions for obtaining parameters. Besides, production practice is mainly based on Dupuit and Thiem to determine the stable flow pumping test formula to determine the impact radius of the diving aquifer, and on this basis extended by the linear plot [2-3].

Nevertheless, both pumping wells and at least one observation well are required for parameters. Making

*e-mail: benisi.hamed@fzu.edu.cn

more and more use of single-hole pumping tests has the advantages of low cost and simpleness. It is worth exploring and studying how to use single-hole no-observation holes to determine hydrogeological parameters to avoid the influence of field conditions.

In recent years, numerical methods have gradually been applied in the test of pumping wells. Zhu and Yeh (2005) applied hydraulic tomography to numerical methods, explaining the spatial distribution of hydraulic parameters of aquifers by inversion [4]. Chen Xiaoyi et al. (2016) calculated the parameters of the aquifer by parsing numerical simulation and obtained the aquifer permeation coefficient value more accurately [5]. Chen Chen et al. (2017) used Aquifer Test data to solve aquifer parameters using pumping test data, which focused on pore permeation coefficients and elastic water supply [6].

The practical applications of the theoretical methods also revealed their limitations in acquiring hydrogeological parameters since the complex and unknown environment in which most projects are located presents significant difficulties to the applicability of the proposed approaches. Consequently, field pumping test is extensively exploited and applied to obtain accurate parameters for relevant problems. Regarding the implementation of field pumping tests, the high cost and low efficiency are still the main limitations in acquiring parameters. For instance, Zhao Ruiyu et al. (2021) still adopted the aquifer superimposed discharge test to describe the spatial distribution of the overall hydrogeological parameters in the study area [7].

In recent years, meshless methods have become increasingly popular. Addressing the shortcomings of the traditional numerical method requires the generation of complex meshes and cumbersome calculation times to arrive at approximate solutions [8]. The Trefftz method can quickly solve the boundary value problem. At present, it has been applied in many fields of physics, mathematics, and engineering, the approximate solution can be expressed as a linear combination of functions that satisfy the control equation [9-18]. Li et al. (2007, 2008) made a comprehensive comparison of Trefftz and other boundary methods to conclude that Trefftz is the simplest method of calculation, providing the most accurate equation solution and optimal numerical stability [19-20]. In 2018, some scholars combined the collocation scheme from the method of fundamental solutions (MFS) with the collocation Trefftz method (CTM) to improve the applicability of the method for solving boundary value problems [21]. For inverse Cauchy problems, Liu (2008) respectively applied indirect and direct Trefftz methods to solve these problems [22-23]. However, they could only calculate more than 50% of the cases with known boundaries and only proposed solutions for single-connected problems. Liu et al. (2013, 2018) used CTM (Collocation Trefftz method) to reduce the known boundary to 40% when solving the simply connected

inverse Cauchy problem, but the unlimited domain and double connected problem was not involved – and related engineering problems [24-25]. Xiao (2018) carried out an application examples of subsurface flow problems with free surface in homogenous and layered heterogeneous geological media to model geofluid flow in heterogeneous geological media [26]. Ku Cheng Yu (2019) utilizing Trefftz functions for modeling subsurface flow problems, obtain the accurate location of the nonlinear moving boundary for transient problems by the superposition theorem using the basis functions [27]. Yang and Su et al. (2020) used Trefftz method and space-time collocation method to simulate the fluctuation characteristics of groundwater in coastal aquifers, but it was only based on one-dimensional homogeneous and isotropic soil, and never involve the groundwater problem of two-dimensional soil [28]. Xi Qiang (2020) introduces a novel localized collocation Trefftz method (LCTM) for potential-based inverse electromyography, the sparse linear system is yield by satisfying governing equation at interior nodes and boundary conditions at boundary nodes and mitigates the ill-conditioning resultant matrix encountered in the CTM [29].

In this paper, we present a New Method based on the infinite domain problem, using Trefftz Method and the New Fictitious Time Integration Method (NFTIM) [30], to determine the aquifer parameters in the actual engineering of the pumping well test problem. This method achieves that in the absence of observation wells and the uncertainty of hydraulic conductivity T and permeability coefficient K, the influence radius R of the submersible aquifer is obtained directly and the approximate head distribution and deep drop in the affected area.

Materials and Methods

Basic Principle

Trefftz Method Class II Boundary Condition Substrate

The two-dimensional Laplace equation is derived from the following expression:

$$\Delta u = \frac{\partial^2 u}{\partial x^2} + \frac{\partial^2 u}{\partial y^2} = 0 \tag{1}$$

The first kind of boundary condition is the constant water head boundary condition (the Dirichlet boundary condition), whose boundary value can be expressed as several stages:

$$f = \sum_{v=1}^{n} \alpha_v \Psi_v \tag{2}$$

Where f denotes the boundary value for the Dirichlet boundary condition, n denotes the total number of items in the expansion, α_v denotes the coefficient obtained from the expansion of order v, Ψ_v is the Dirichlet boundary condition T-complete basis.

By simplifying the Dirichlet boundary condition, the 2D Laplace Formula T-complete basis function can be organized

$$\{1, \ln r, r^v \cos v\theta, r^v \sin v\theta, r^{-v} \cos v\theta, r^{-v} \sin v\theta\} \quad (3)$$

By adding legal rationale to the Trefftz basis line overlay to control equation, approximate solution at the Dirichlet boundary condition can be expressed as follows:

$$u = a_0 + b_0 \ln r + \sum_{v=1}^{m} \left[(a_v r^v + b_v r^{-v}) \cos v\theta + (c_v r^v + d_v r^{-v}) \sin v\theta \right] \quad (4)$$

Where the solution u is the approximated solution at the collocation point, t donates the distance between the setting point and the source point, and θ donates the included angle between the line connecting the setting point and the source point and the positive direction of the polar axis, m donates the total order of Trefftz method. For determining the coefficients such as a_0, b_0, a_v, b_v, c_v, d_v, we must employ the collocation method.

The second type of boundary condition is the flux boundary condition (the Neumann boundary condition), whose boundary flux can first be expanded by the number of stages as follows:

$$g = \sum_{v=1}^{n} \overline{\alpha}_v \overline{\Psi}_v \quad (5)$$

Where g denotes the boundary flux for the Neumann boundary condition, n denotes the total number of items in the expansion, $\overline{\alpha}_v$ is equal to α_v when we solve the same problem, $\overline{\Psi}_v$ denotes the Neumann boundary condition T-complete basis.

By simplifying the Neumann boundary condition, the 2D Laplace Formula T-complete basis function can be organized

$$\begin{aligned}
&\{\frac{1}{r}(\cos\theta n_x + \sin\theta n_y), [(vr^{v-1}\cos v\theta\cos\theta + vr^v \sin v\theta \frac{\sin\theta}{r})n_x \\
&+ (vr^{v-1}\cos v\theta\sin\theta - vr^v \sin v\theta \frac{\cos\theta}{r})n_y], [(vr^{-v}\sin v\theta \frac{\sin\theta}{r} \\
&- vr^{-v-1}\cos v\theta\cos\theta)n_x + (-vr^{-v}\sin v\theta \frac{\cos\theta}{r} - vr^{-v-1}\cos v\theta\sin\theta)n_y] \\
&, [(vr^{v-1}\sin v\theta\cos\theta - vr^v \cos v\theta \frac{\sin\theta}{r})n_x + (vr^{v-1}\sin v\theta\sin\theta \\
&+ vr^v \cos v\theta \frac{\cos\theta}{r})n_y], [(vr^{-v}\cos v\theta \frac{\sin\theta}{r} - vr^{-v-1}\sin v\theta\cos\theta)n_x \\
&+ (-vr^{-v}\cos v\theta \frac{\cos\theta}{r} - vr^{-v-1}\sin v\theta\sin\theta)n_y]\}
\end{aligned} \quad (6)$$

Linear superposition of the Trefftz basis by addition theorem, and the result of the control equation differential when the Neumann boundary condition is differentially derived, can be represented as follows:

$$\begin{aligned}
\frac{\partial u}{\partial n} = b_0 \frac{1}{r}(\cos\theta n_x + \sin\theta n_y) + \\
\sum_{v=1}^{m} \left\{ \begin{array}{l}
a_v v[(r^{v-1}\cos v\theta\cos\theta + r^{v-1}\sin v\theta\sin\theta)n_x \\
+ (r^{v-1}\cos v\theta\sin\theta - r^{v-1}\sin v\theta\cos\theta)n_y] \\
+ b_v v[(r^{-v-1}\sin v\theta\sin\theta - r^{-v-1}\cos v\theta\cos\theta)n_x \\
+ (-r^{-v-1}\sin v\theta\cos\theta - r^{-v-1}\cos v\theta\sin\theta)n_y] \\
+ c_v v[(r^{v-1}\sin v\theta\cos\theta - r^{v-1}\cos v\theta\sin\theta)n_x \\
+ (r^{v-1}\sin v\theta\sin\theta + r^{v-1}\cos v\theta\cos\theta)n_y] \\
+ d_v v[(r^{-v-1}\cos v\theta\sin\theta - r^{-v-1}\sin v\theta\cos\theta)n_x \\
+ (-r^{-v-1}\cos v\theta\cos\theta - r^{-v-1}\sin v\theta\sin\theta)n_y]
\end{array} \right\}
\end{aligned} \quad (7)$$

Two-dimensional Laplace problems can be simply divided into simply connected domain problems, infinite domain problems and multiply connected domain problems. In this manuscript, the problem of pumping well test is an infinite domain problem, the calculation domain is infinite in scope, and there is a cavity in the domain. When solving, the source point is placed in the cavity in the defined domain, and its calculation model is shown in Fig. 1. At this point, the T-complete base is represented as:

$$\{\ln r, r^{-1}\cos\theta, r^{-1}\sin\theta, \dots, r^{-v}\cos v\theta, r^{-v}\sin v\theta\} \quad (8)$$

New Fictitious Time Integration Method (NFTIM)

In this manuscript, the NFTIM is introduced, improving the accuracy; stability of the numerical method; and reducing the calculation time effectively [30]. Moreover, solving nonlinear equations can make the physical significance more precise, ignore the Jacobian matrix derivative, and effectively improve the morbid problem.
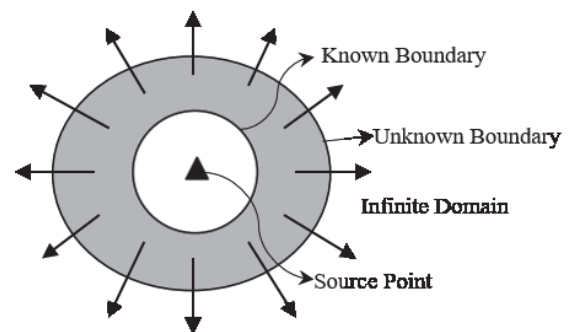

Fig. 1. Diagram of two-dimensional Laplace infinite domain problem.

First, consider a nonlinear algebraic array such as

$$F_i(x_i, \dots, x_N) = 0, i = 1, \dots, N \tag{9}$$

Introduce a virtual time parameter τ, assuming a time-related function

$$y_i(\tau) = (1 + \tau)x_i \tag{10}$$

The control parameter $\Re$ is introduced, and the former difference method is used for integration. It can be obtained that

$$x_i^{K+1} = x_i^K - \frac{H\Re}{1 + \tau_K} F_i(x_i^K, \dots, x_N^K) \tag{11}$$

H denotes the fictitious time step, K denotes the Kth discrete, τ_K denotes accumulation of the fictitious time $\tau_K = KH$.

Eq. (11) NFTIM solves the numerical time integral formula of linear equations and nonlinear equations.

Virtual time function in the method $q(\tau) = 1 + \tau$, three conditions have to be met:
(1) $q(\tau)$ must be a differentiable function;
(2) $q(0) = 1$;
(3) $q(\infty) = \infty$.

Based on this, a new virtual time function with a broader meaning is proposed, which can effectively improve the stability of solving highly nonlinear problems:

$$q(\tau) = (1 + \tau)^w, 0 \le w \le 1 \tag{12}$$

Where w denotes the fictitious time parameter, can rewrite the Eq. (10) to

$$y_i(\tau) = (1 + \tau)^w x_i \tag{13}$$

than

$$\dot{x}_i = -\frac{\Re}{(1 + \tau)^w} F_i(x_i, \dots, x_N) \tag{14}$$

The difference method of the preceding item is used to integrate Eq. (14), can be expressed as

$$x_i^{K+1} = x_i^K - \frac{H\Re}{(1 + \tau_K)^w} F_i(x_i^K, \dots, x_N^K) \tag{15}$$

H denotes the fictitious time step, w denotes the fictitious time parameter, K denotes the Kth discrete, τ_K denotes accumulation of the fictitious time, and $\tau_K = KH$. Eq. (15) is the numerical time integral formula for solving linear equations and nonlinear equations by NFTIM.

Calculation Process

Modeling and Matching Points

Groundwater control equation, or Laplace equation

$$\frac{\partial^2 u}{\partial x^2} + \frac{\partial^2 u}{\partial y^2} = 0 \tag{16}$$

Given the calculation domain and the initial condition

$$\Gamma_D : u(x, y) = f(x, y) \tag{17}$$

$$\Gamma_N : \frac{\partial u(x, y)}{\partial n} = g(x, y) \tag{18}$$

Where $f(x, y)$ denotes the first kind of boundary condition function of the constant head, $g(x, y)$ denotes the second kind of boundary condition function of constant flow, it is assumed that both the Dirichlet and the Neumann boundary conditions are satisfied.

As shown in Fig. 2, N points are arranged on the boundary of a given computing domain Ω. The specific location of boundary points $1 \sim n_1$ is known. The position of boundary points $n_1 + 1 \sim n_1 + n_2$ is unknown; convert rectangular coordinate system (x_i, y_i) to the cylindrical coordinate system (r_i, θ_i).

Solve the Pending Coefficients

According to the given boundary conditions above, the collocation points at each known position are respectively substituted into the boundary condition functions of class 1 of constant head $f(x, y)$ and class 2 of constant flow $g(x, y)$. The accurate boundary value calculated is substituted into Eqs (4) and (7), and all the boundary points at known positions can be jointly established into a set of linear algebraic equations. We introduce the characteristic length R_0 to improve the accuracy of the solution while maintaining the stability of the matrix [31].
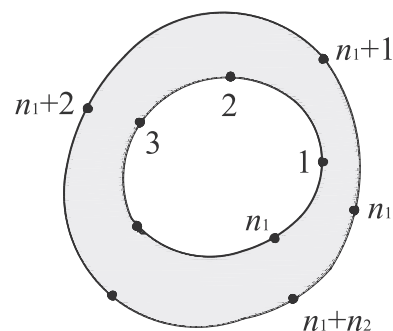

Fig. 2. Schematic diagram of Trefftz inverse calculation model.

Considering the Dirichlet boundary condition of constant head, the approximate solution is shown as follows:

$$b_0 \ln r_i + \sum_{v=1}^{m} \left[b_v (\frac{r_i}{R_0})^{-v} \cos v\theta_i + d_v (\frac{r_i}{R_0})^{-v} \sin v\theta_i \right] = f(x_i, y_i)$$

(19)

Considering the Neumann boundary condition of constant flow, the approximate solution is shown as follows:

$$b_0 \frac{1}{r_i} (\cos\theta_i n_{x_i} + \sin\theta_i n_{y_i}) + \sum_{v=1}^{m} (b_v NA_v^{r_i} + d_v NB_v^{r_i}) = g(x_i, y_i)$$

(20)

where

$$NA_v^{r_i} = \{[(-vr_i^{-v-1}R_0^{\ v} \cos v\theta_i \cos\theta_i + vr_i^{-v-1}R_0^{\ v} \sin v\theta_i \sin\theta_i) n_{xi}]$$
$$+ [(-vr_i^{-v-1}R_0^{\ v} \cos v\theta_i \sin\theta_i - vr_i^{-v-1}R_0^{\ v} \sin v\theta_i \cos\theta_i) n_{yi}]\}$$

(21)

$$NB_v^{r_i} = \{[(-vr_i^{-v-1}R_0^{\ v} \sin v\theta_i \cos\theta_i - vr_i^{-v-1}R_0^{\ v} \cos v\theta_i \sin\theta_i) n_{xi}]$$
$$+ [(-vr_i^{-v-1}R_0^{\ v} \sin v\theta_i \sin\theta_i + vr_i^{-v-1}R_0^{\ v} \cos v\theta_i \cos\theta_i) n_{yi}]\}$$

(22)

The linear algebraic equations jointly established at all known boundary points can be expressed as the matrix operation form of $A\alpha = B$:

$$A = \begin{bmatrix} \ln r_1 & (\frac{r_1}{R_0})^{-1}\cos\theta_1 & (\frac{r_1}{R_0})^{-1}\sin\theta_1 & \cdots & (\frac{r_1}{R_0})^{-v}\cos v\theta_1 & (\frac{r_1}{R_0})^{-v}\sin v\theta_1 \\ \vdots & \vdots & \vdots & \ddots & \vdots & \vdots \\ \ln r_{n_1} & (\frac{r_{n_1}}{R_0})^{-1}\cos\theta_{n_1} & (\frac{r_{n_1}}{R_0})^{-1}\sin\theta_{n_1} & \cdots & (\frac{r_{n_1}}{R_0})^{-v}\cos v\theta_{n_1} & (\frac{r_{n_1}}{R_0})^{-v}\sin v\theta_{n_1} \\ \frac{1}{r_1}(\cos\theta_1 n_{x_1} + \sin\theta_1 n_{y_1}) & NA_1^{r_1} & NB_1^{r_1} & \cdots & NA_v^{r_1} & NB_v^{r_1} \\ \vdots & \vdots & \vdots & \ddots & \vdots & \vdots \\ \frac{1}{r_1}(\cos\theta_{n_1} n_{x_{n_1}} + \sin\theta_{n_1} n_{y_{n_1}}) & NA_1^{r_{n_1}} & NB_1^{r_{n_1}} & \cdots & NA_v^{r_{n_1}} & NB_v^{r_{n_1}} \end{bmatrix}$$

$$\alpha = [b_0, b_1, d_1 \ldots b_v, d_v,]^T \qquad B = [f_1, \ldots, f_{n_1}, g_1, \ldots, g_{n_1}]^T$$

(23)

Where A is an $aa \times bb$ matrix composed of Trefftz basis functions, B is an $aa \times 1$ vector composed of boundary values. The pending factor α is an $bb \times 1$ vector, and $aa = 2n_1$, $bb = 2m + 1$.

Due to the Trefftz basis function is derived from the groundwater control equation, and the Trefftz method itself has strong stability and is not susceptible to disturbance, so as long as the boundary point of partially known locations can meet the boundary conditions well, the pending coefficient can be solved by the left division operation in Matlab program

$$\alpha = A/B$$

(24)

Calculate the Location of the Unknown Boundary

Use polar coordinate systems (r_i, θ_i), θ_i of $n_1 + 1 \sim n_1 + n_2$ boundary points with unknown boundaries can be set to known values. Only r_i is needed to determine each point's specific position to determine the shape of unknown boundaries.

Assuming that $r_i = r_0$, r_0 donates initial guess value, according to the obtained undetermined coefficient vector α, substitute the Dirichlet boundary condition and the Neumann boundary condition basis function to obtain the matrix operation form of $A'\alpha = B'$

$$A' = \begin{bmatrix} \ln r_i & (\frac{r_i}{R_0})^{-1}\cos\theta_i & (\frac{r_i}{R_0})^{-1}\sin\theta_i & \cdots & (\frac{r_i}{R_0})^{-v}\cos v\theta_i & (\frac{r_i}{R_0})^{-v}\sin v\theta_i \\ \frac{1}{r_i}(\cos\theta_i n_{x_i} + \sin\theta_i n_{y_i}) & NA_1^{r_i} & NB_1^{r_i} & \cdots & NA_v^{r_i} & NB_v^{r_i} \end{bmatrix}$$

$$B' = [f_i', g_i']^T$$

(25)

The polar coordinate system (r_i, θ_i) of the unknown boundary points is converted into a Cartesian coordinates system (x_i, y_i), and substituted into Eqs. (17), (18) to obtain f_i and g_i. The error δ of the unknown boundary points is calculated. If the error is less than the convergence precision, then (r_i, θ_i) is the desired position point.

$$\delta = \max\left\{ |f'_i - f_i|, |g'_i - g_i| \right\}$$

(26)

If the error is greater than the convergence accuracy, The NFTIM needs to quickly find the r_i satisfying condition. At this point, the newly assumed r_i can be obtained by the following equation

$$r_i^{K+1} = r_i^K - \frac{H\Re}{(1 + \tau_K)^w} \delta$$

(27)

Where H denotes the fictitious time step, w denotes the fictitious time parameter, K denotes the Kth discrete, τ_K denotes accumulation of the fictitious time, and $\tau_K = KH$.

Then, matrix calculation is carried out for the newly assumed r_i, and the convergence accuracy is compared until the error is less than the convergence accuracy. At this time, (r_i, θ_i) is the desired position point. As long as the points are dense enough, all the calculated position points can be combined to obtain the shape of all the unknown boundaries.

The exact calculation steps are shown in Fig. 3.

Calculate the Internal Point Water Head Value

Substituting the undetermined coefficient into the approximate solution composed of the Trefftz basis, the corresponding water head value $u(x_i, y_i)$ can be
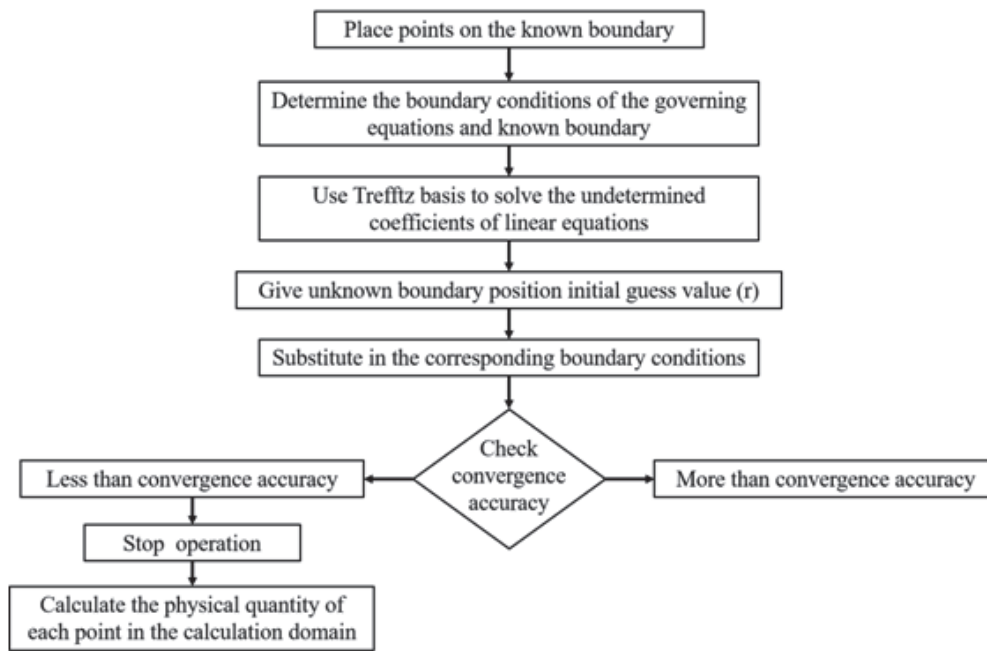
Fig. 3. Calculate the flowchart.

calculated from **B** = **Aα** any point in the calculation domain.

$$u(x_i, y_i) = b_0 \ln r_i + \sum_{v=1}^{m} \left[b_v (\frac{r_i}{R_0})^{-v} \cos v\theta_i + d_v (\frac{r_i}{R_0})^{-v} \sin v\theta_i \right]$$

(28)

We should pay attention to whether the internal water head value meets the actual physical phenomenon. The accuracy of the undetermined coefficient vector **α**

obtained by partial known boundary should be initially determined.

Case Study

Engineering Overview

Harbin is located in the central and southern part of Heilongjiang Province, which belongs to the Songnen Plain. The overall terrain is relatively flat, and the
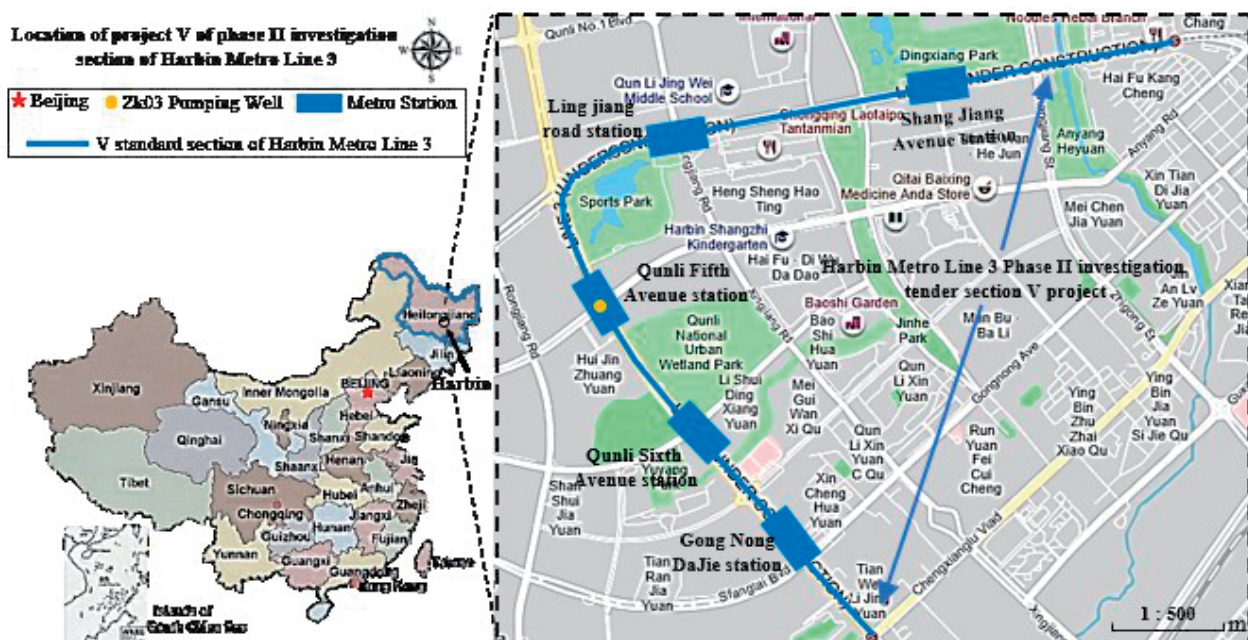

Fig. 4. Study area section V of phase II investigation of Harbin Metro Line 3.

landforms are mainly flowing water landforms. The famous Songhua River runs through Harbin from west to east. Harbin Metro Line 3 belongs to the second phase of the project [32]. The mainline has a total length of about 32 km, with all underground lines and underground stations. Survey the V section of 6 stations, with a total length of the line about 6.37 km. There are nine drilling holes and two observation holes for pumping tests in Section V of the Phase II engineering survey. The engineering data used in this case is from hole ZK03 of Qunli Fifth Avenue Station, Section V of Phase II engineering survey of Line 3, with an observation hole attached, as shown in Fig. 4. After well completion, a steady flow pumping test will be carried out. The water pumping test hole has a diameter of 400 mm and a depth of 47-56 m after good completion, penetrating the Quaternary strata. The observation hole has a diameter of 108 mm and a depth of 35 m.

The engineering area belongs to the submersible groundwater, water-conducting, water-rich, rock permeability gradually increases with the particles thickening from top to bottom, weighted average penetration coefficient is 18.85~33.21 *m/d*, inferred water inflow is 3000~5000 *m³/d*. According to the formation lithology extracted during drilling, the measured data of initial water level and stable water level, as well as the average permeability coefficient of the aquifer of hole ZK01, as shown in Table 1, the permeability coefficient of hole ZK03 selected in Qunli Fifth Avenue Station in this study can be estimated to be 20.17 *m/d*.

The engineering situation of the Zk03 hole in the V standard section of Harbin Metro Line 3 is summarized into the following parameter table for subsequent calculation and analysis as shown in Table 2:

Model Building

This case study area is an infinite domain problem with the following shape parameters:

$$\Omega = \{(x, y) | x = \rho(\theta)\cos\theta, y = \rho(\theta)\sin\theta\}$$
$$0 \leq \theta \leq 2\pi \tag{29}$$

$$r(\theta) \geq 0.2 \tag{30}$$

Two-dimensional homogeneity steady state control equation:

$$\Delta h(x, y) = 0 \tag{31}$$

The problem of pumping wells usually involves only the boundary of the head, all the boundaries, in this case, meet the Dirichlet boundary conditions, and the specific boundary conditions are set as follows:

$$h(x, y) = 108.50m \qquad (x, y) \in \Gamma_1 \tag{32}$$

$$h(x, y) = 111.05m \qquad (x, y) \in \Gamma_2 \tag{33}$$

According to the Thiem formula, set the analytical solution expression to

$$h = \frac{Q}{2\pi T}\ln r + C \tag{34}$$

Table 1. Zk03 single-hole pumping test, observation hole layout table.

Main hole number	Observation hole	Observe the borehole diameter (mm)	Observe the depth of the hole (m)	Illustrate
Zk03	C2	108	35	Away from the main hole 15 m

Table 2. Zk03 pumping test data table.

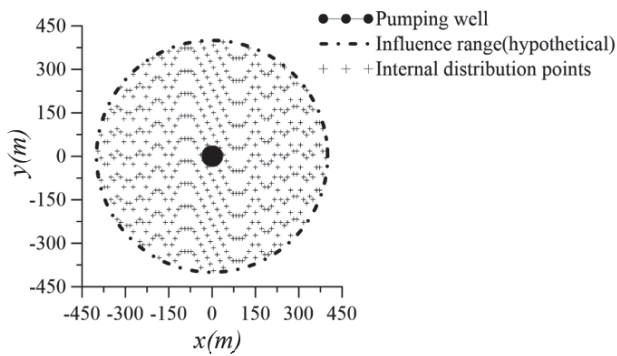| Parameter	Unit	Value	Comment
Water level /Buried deep	*m*	111.05/7.2	Dalian elevation
Pumping well radius r_w	*m*	0.2	\
Observation wells and Pumping wells distance	*m*	15	\
Aquifer thickness	*m*	34	Cumulative thickness
Quantity of flow Q	*m³/h*	50	\
Main well deep	*m*	2.55	\
Observation wells Drop deep	*m*	1.76	\
Permeability coefficient k	*m/d*	20.17	\

Fig. 5. Boundary and interior points layout diagram.

where

$$C = h_{C2} - \frac{Q}{2\pi bk} \ln r_{C2} \quad (35)$$

and

$$h = \frac{Q}{2\pi bk} \ln \frac{r}{r_{C2}} + h_{C2} \quad (36)$$

This case considers configuring 400 boundary points evenly distributed on the boundary, of which 200 points are known internally, and 200 points are unknown external boundaries. The order of the selected basis function is 20, and the position and range are shown in Fig. 5 and the radius of the impact range in the figure is hypothetical. Because the location of the outer boundary is unknown, the internal point spacing configured within the calculation domain is 2, and the details of each parameter are detailed in Table 3.

Results and Discussion

Observation Well Verification

First of all, we use the Trefftz method to reverse the verification of the location of the observation well under the condition that the inside is the pumping well head, to verify the feasibility of this method in the pumping

well experiment, at this time, the boundary condition of the unknown boundary is

$$h(x, y) = 110.03m \qquad (x, y) \in \Gamma_2 \quad (37)$$

The location of unknown observation wells is restored using the Trefftz method in the known pumping well location and the stable pumping head boundary conditions, as shown in Fig. 6. It can be concluded from the figure that the boundary position of the calculated water head of 110.03m is highly coincident with the position of $r = 15m$ the observation well, indicating that the recovered observation well position fits with the height of the correct observation position. The result of the recovery boundary is calculated with an absolute error of the correct boundary, as shown in Fig. 7, θ donates angle of unknown boundary points. The absolute error between the restored boundary position and the correct boundary was 9.94×10^{-10}, which shown a very considerable accuracy. The calculation parameters are illustrated in Table 4.

Next, the case is parsed and verified with the Thiem formula. Specifically, under the Dirichlet boundary conditions, the known boundary is only the inner boundary, the location range of the pumping well, and the head height. The Trefftz method is used to calculate the numerical solution in the domain, and it is compared with the Thiem formula for the analytical solution. A total of 522,459 internal points are arranged by the distance of 1m from the shaft of the pumping well. Fig. 8 shows the error distribution of numerical and analytical solutions, where the calculation domain is from the known inner boundary of the pumping well to the unknown outer boundary of the observation well. From the figure, it can be seen that the maximum absolute error of the two is 3.52×10^{-18}. The error fluctuations are concentrated near the inner boundary and farther away from the inner boundary; absolute error is flattened. The error distribution is uniform and maintained at 10^{-18} under the high precision range. There is no convergence, indicating that the pumping well test in using the Trefftz method compared to the Thiem formula is comparable, with a high degree of accuracy.

Table 3. Pumping well test calculates the model parameter table.

parameter	Space boundary points	Known boundary points	Internal point spacing	Order
Value	400	200	1	20

Table 4. Pumping well test observation well verification simulation parameter table.

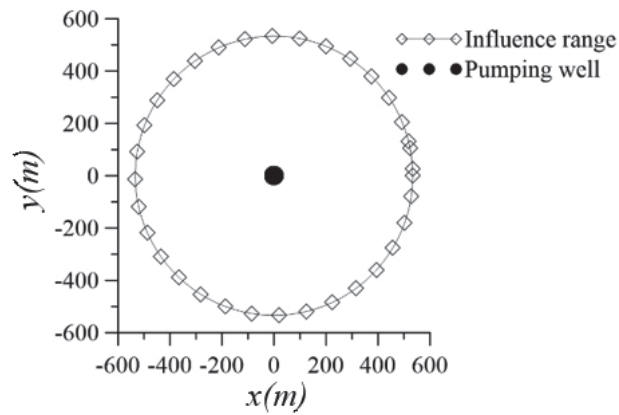| Project	Initial guess	Convergence steps	Convergence condition	Fictitious time steps H	Control parameters $\Re$	Time parameter w
Parameter	10	2333	10^{-9}	0.8	1	0.1

Fig. 6. Observation well boundary recovery check diagram.

Fig. 7. Observation well checking boundary absolute error diagram.

Fig. 8. An absolute error distribution map of analytical and numerical solutions in an observation well domain.
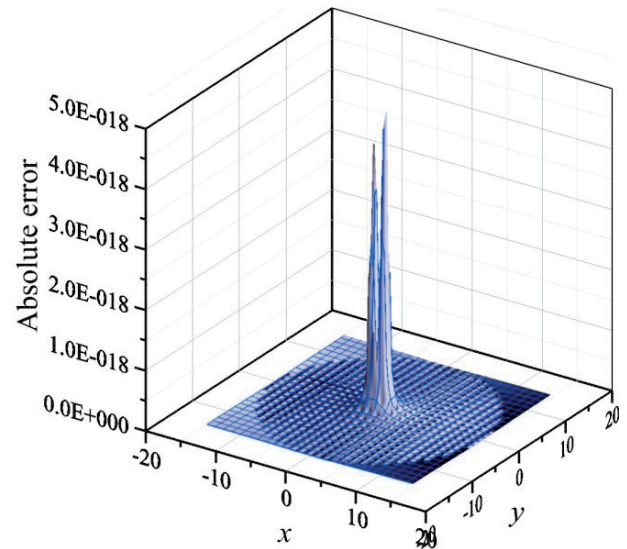

Fig. 9. Impact range boundary diagram.
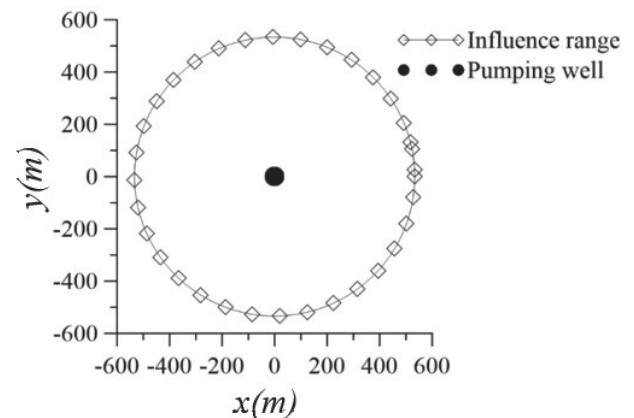
Impact Radius

After verifying the feasibility of the calculation and proof method within the observation well, the radius of the impact range of the pumping well is calculated. The impact radius is the distance from the shaft of the pumped well to the groundwater level drop of zero, which is a constant value, and a distance can simply express the impact radius.

When calculating the impact radius, the known inner boundary is still the head of the pumping well, and the Trefftz method is used for the reverse calculation of the influence radius. In this case, the boundary condition of the unknown boundary is the elevation of the original water head of the pumping well

$$h(x, y) = 111.05m \qquad (x, y) \in \Gamma_2 \tag{38}$$

Details of parameters calculated for the radius of influence of the pumping well test are shown in Table 5. Because two decimal places are reserved for the test data, the boundary convergence condition is set as 10^{-2}, that is, three decimal places are reserved to ensure the validity of the calculation results. Data retention will be discussed again in the following paper.

As shown in Fig. 9, the unknown boundary is restored to find the radius of the impact range

Table 5. Calculation and simulation parameter table of influence radius of pumping well test.

Project	Initial guess	Convergence steps	Convergence condition	Fictitious time steps H	Control parameters $\Re$	Time parameter w
Parameter	300	2659	10^{-2}	2	2	0.1

of the pumping well, as can be seen from the figure, the impact radius of the pumping well is 563.81 m.

Drop Deep

After drawing a diagram of the boundaries of the impact range of the entire pumping well, we calculated the head value within the range of the impact radius, in which an internal point was arranged 1m apart from the shaft of the pumping well, with a total of 988048 internal points. The results of the distribution of the head within the range were calculated as shown in Fig. 10, the cross represents the depth reduction at a certain distance from the pumping well axis, and the line represents the fitting curve of the depth reduction at each point. From the figure, it can be seen that the closer the distance from the shaft of the pumping well, the faster the head changes, the smaller the change of the head when the influence radius is more significant.

After obtaining a diagram of the overall distribution of the head in the range, When $\theta = 0$ is selected, the relationship between the height of water level drop when the distance R from the axis of the pumping well increases is obtained, that is, the drop deep curve. As shown in Fig. 11, when the distance from the axis of the pumping well is less than 50 m, the depth reduction changes significantly; when the distance is greater

than 100 m, the water level begins to decline slowly at a certain speed. When the distance exceeds 450 m, the water level changes little, and the overall law conforms to the objective fact.

Next, we try to verify the analytical solution with Thiem formula. Specifically, under the Dirichlet boundary conditions, the known boundary is only the inner boundary, the location range of the pumping well, and the head height. Trefftz method is used to calculate the numerical solution in the domain, compared with the Thiem formula. Fig. 12 shows the error distribution of numerical and analytical solutions within the influence range, where the calculation area is from the known inner boundary of the pumping well to the outer boundary of the unknown impact radius. It can be seen from the figure that the maximum absolute error of the two is 1.11×10^{-15}, and the error fluctuation is evident in the calculation domain. The error fluctuation is the largest near the pumping well. However, the error always remains within the accuracy of $7 \times 10^{-16} \sim 1 \times 10^{-15}$. There is no non-convergence, which indicates that the Thiem formula is verifiable in this kind of problem.

Although Thiem formula is also applicable to the single-well pumping problem, it can be seen from Eq. (39) that the constant C must be determined first

$$h = \frac{Q}{2\pi T} \ln r + C \tag{39}$$

To confirm the constant C, an observation well must be present, and the distance from the observation well to the pumping well must be accurately measured. The water level of the observation well after the pumping is stable. The deformation of Eq. (39) is transformed into Eq. (40).
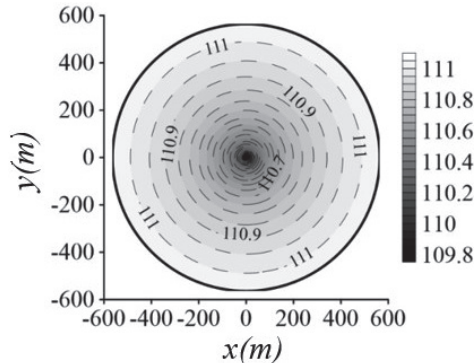

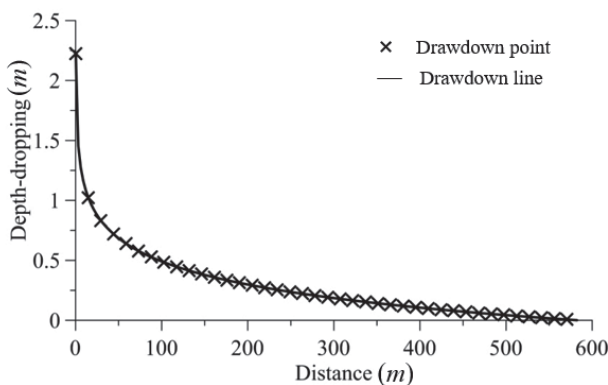Fig. 10. Water head distribution diagram.
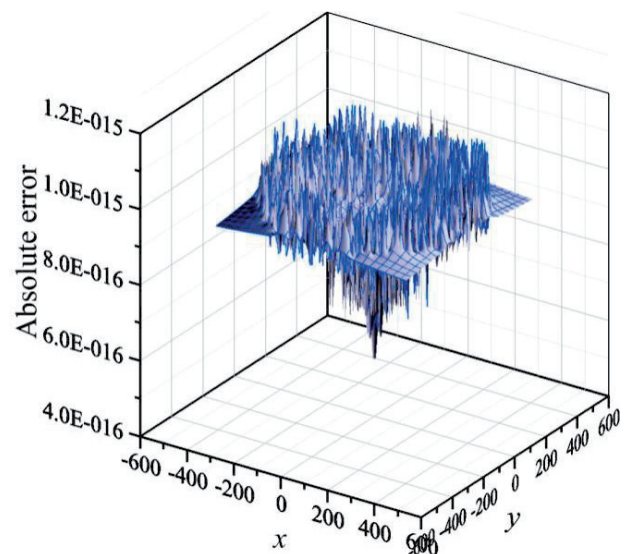

Fig. 11. Depth-dropping graph.

Fig. 12. Absolute error distribution diagram of analytic and numerical solutions within the influence range.

$$h = \frac{Q}{2\pi T} \ln \frac{r}{r_0} + h_0 \qquad (40)$$

At this point, water head, depth drop and other parameters can be calculated at any point within the calculation range. However, in actual engineering, due to the limited site conditions, it is sometimes impossible to carry out borehole observation. Secondly, when the impact radius range of the pumping well is uncertain, the validity of the borehole location of the observation well cannot be confirmed. If the distance is too close to the pumping well will cause large error. However, if the distance is too far, the water level will change too little or even remain unchanged beyond the impact radius range, resulting in the failure of the data of the observation well. In addition, drilling work has a certain cost. Therefore, by comparison, the Trefftz method can highlight the advantages of the inverse calculation of pumping well problems. It is more practical and effective to complete the regional head calculation and estimate the boundary of the affected area without the existence of the observation well and with higher accuracy.

Engineering Impact Assessment

Due to the engineering measurement error, the experimental data is reserved to two decimal places, and the calculation is used to reserve three decimal places for reference. In actual engineering, if two decimal places are retained, the impact radius of the pumping well can be regarded as 408.20 m. The depth drop here is less than 0.1 m, so it can be basically regarded as the influence radius of the pumping well. The reference range of the given influence radius is 331~538 m according to the real pumping test, and 408 m is calculated. The results are in good agreement with those calculated in this paper.

According to the above data, the water flow in the working area of the test site affected the overall topography, landform and stratigraphic lithology of the area. The exploration found that there were silty clay, fine sand, medium sand, coarse sand, and gravel in the strata. At the same time, the superior water system conditions bring abundant groundwater. The characteristics of the thick aquifer, strong water permeability, and groundwater depth make foundation pit dewatering work necessary for constructing primary buildings such as the subway. In foundation pit dewatering, the original underground water flow field will be changed, resulting in water head difference. In addition, under the influence of dynamic water pressure itself, fine soil particles will flow through the pores of larger particles under scouring, forming potential erosion, leading to the destruction of regional soil structure, and even the formation of underground quicksand.

Subway occupies most of itself because of the part below the groundwater level. Considering that the groundwater will have a significant buoyancy effect on the foundation, the design should be prepared to deal with the floating effect of groundwater on the whole region under long-term adverse conditions. Therefore, an anti-floating calculation should be carried out.

Conclusions

Taking the V standard paragraph of Harbin Metro Line 3 as a typical case study, using the real data of Zk03 hole pumping test to model, comparing the real data by parsing and verification, and calculating the hydrogeological parameters such as the influence radius, head distribution and depth curve of the pumping well, provide hydrogeological parameters for the design and construction of subway projects.

(1) In this paper, the multilinear equation is transformed into a monistic nonlinear equation to solve the problem of the deformation of the Laplace equation Cauchy problem, and explore the numerical algorithm error estimation to achieve the optimal order. The calculation process and step design of the groundwater inverse problems are carried out by the Trefftz method complete basis function under the Dirichlet and Neumann boundary conditions and combined with the NFTIM.

(2) This paper verifies that the NFTIM method has improved the computational accuracy compared with the traditional iterative method. It has more evident advantages in the problem of the large and complex computational workload. The possibility of calculating the impact range of pumping wells is verified by the case of rule-type infinite domain inverse calculation. The results show that the maximum absolute error between the numerical solution and the analytical solution is less than 10^{-15}. The error fluctuation mainly concentrates near the area where the unknown boundary distribution points are concentrated.

(3) The method presented in this paper was applied to an actual case of pumping well in Section V of Harbin Metro Line 3. Through analytical solution verification with the Thiem formula, the maximum absolute error of the water head in the region is less than 10^{-17}, and the error fluctuation is mainly concentrated near the inner boundary. Secondly, the absolute error is less than 10^{-9} compared with the observed well location, proving that the Trefftz inverse calculation method is more maneuverable and has a high degree of accuracy.

Acknowledgments

University and Heilongjiang College for their technical support.

Conflict of Interest

The authors declare no conflict of interest.

References

1. FENG W. Study on some problems of hydrogeology of unconsolidated aquifer. Doctor degree, University of Geosciences, Beijing, **2018** [In Chinese].

2. WANG J.F., WANG F. The influence radius and environmental influence range of falling funnel of pumping water are discussed. Journal of Hydraulic Engineering, **51** (07), 827, **2020** [In Chinese].

3. ZHAO Z.Z., LU S. The application of Jacob linear graphic method in the pumping test of shengsi 2 well. Jilin Water Resources, **01**, 43-47, **2013** [In Chinese].

4. ZHU J.F., YEH T.C.J. Characterization of aquifer heterogeneity using transient hydraulic tomography. Water Resources Research, **41** (7), **2005**.

5. CHEN X.L., WEN Z., HU J.S., MIN Z.Y., LIANG X., SUN R.B., LI R.C. The analytical method and numerical method are used in the evaluation of the effect of impermeable wall in hydropower station. Editorial Committee of Earth Science Journal of China University of Geosciences, **41** (04), 701, **2016** [In Chinese].

6. CHEN C., WEN Z., LIANG X., LI X. Inversion of hydrogeological parameters of typical aquifers in Jianghan Plain. Editorial Committee of Earth Science Journal of China University of Geosciences, **42** (05), 727, **2017** [In Chinese].

7. ZHAO R.Y., MAO D.Q., LIU Z.B., JI Z.K., CAO Z.B. An analysis of sequential water releasing tests of the confined aquifers in a coal mine based on hydraulic tomography. Hydrogeology & Engineering Geology, **48** (1), 1, **2021**.

8. LIU C.Y., KU C.Y., XIAO J.E., YEIH W. A novel spacetime collocation meshless method for solving two-dimensional backward heat conduction problems. Comp. Model. Eng. Sci., **118**, 229, **2019**.

9. KUO C.L., YEIH W., LIU C.S., CHANG J.R. Solving Helmholtz equation with high wave number and ill-posed inverse problem using the multiple scales Trefftz collocation method. Engineering Analysis with Boundary Elements, **61**, 145, **2015**.

10. LIU C.S. A multiple/scale/direction polynomial Trefftz method for solving the BHCP in high-dimensional arbitrary simply-connected domains. International Journal of Heat and Mass Transfer **92** (JAN.), 970, **2016**.

11. KU C.Y. On solving three-dimensional Laplacian problems in a multiply connected domain using the multiple scale Trefftz method. CMES: Computer Modeling in Engineering & Sciences, **98** (5), 509, **2014**.

12. KU C.Y., KUO C.L., FAN C.M., LIU C.S., GUAN P.C. Numerical solution of three-dimensional Laplacian problems using the multiple scale Trefftz method. Engineering Analysis with Boundary Elements, **50**, 157, **2015**.

13. MIERZWICZAK M., KOODZIEJ J.A. Comparison of three meshless methods for 2D harmonic and biharmonic problems. Engineering Analysis with Boundary Elements, **118**, 157, **2020**.

14. MIERZWICZAK M., FRASKA A., GRABSKI J.K. Determination of the Slip Constant in the Beavers-Joseph Experiment for Laminar Fluid Flow through Porous Media Using a Meshless Method. Mathematical Problems in Engineering, **2019**, **2019**.

15. FAN C.M., LI H.H., HSU C.Y., LIN C.H. Solving inverse Stokes problems by modified collocation Trefftz method. Journal of Computational & Applied Mathematics, **268**, 68, **2014**.

16. FAN C.M., LI H.H. Solving the inverse Stokes problems by the modified collocation Trefftz method and Laplacian decomposition. Applied Mathematics & Computation, **219** (12), 6520, **2013**.

17. LV H., HAO F., WANG Y., CHEN C.S. The MFS versus the Trefftz method for the Laplace equation in 3D. Engineering Analysis with Boundary Elements, **83** (oct.), 133, **2017**.

18. TREFFTZ E. Ein Gegenstuck zum Ritzschen Verfahren. In: Proceedings of the 2nd International Congress for Applied Mechanics, Zurich, 131, **1926**.

19. LI Z.C., LU T.T., HUANG H.T., CHENG A.H.D. Trefftz, collocation, and other boundary methods – A comparison. Numer Methods Partial Differential Equations, **23** (1), 93, **2007**. doi:10.1002/num.20159.

20. LI Z.C., LU T.T., HU H.Y., CHENG A.H.D. Trefftz and collocation methods. WIT Press, Southampton/Boston, 432, **2008**.

21. XIAO J.E., KU C.Y., HUANG W.P., SU Y., TSAI Y.H. A Novel Hybrid Boundary-Type Meshless Method for Solving Heat Conduction Problems in Layered Materials. Applied Sciences, **8** (10), **2018**.

22. LIU C.S. A modified collocation Trefftz method for the inverse Cauchy problem of Laplace equation. Engineering Analysis with Boundary Elements, **32** (9), 778, **2008**.

23. LIU C.S. A highly accurate MCTM for inverse Cauchy problems of Laplace equation in arbitrary plane domains. Computer Modeling in Engineering & Sciences, **35** (2), 91, **2008**.

24. LIU C.S., ATLURI S.N. Numerical solution of the Laplacian Cauchy problem by using a better postconditioning collocation Trefftz method. Engineering Analysis with Boundary Elements, **37** (1), 74, **2013**.

25. LIU C.S., CHEN Y.W., CHANG J.R. The Trefftz test functions method for solving the generalized inverse boundary value problems of Laplace equation. Journal of Marine Science and Technology (Taiwan), **26** (5), 638, **2018**.

26. XIAO J.E., KU C.Y., LIU C.Y., YEIH W.C. A Novel Boundary-Type Meshless Method for Modeling Geofluid Flow in Heterogeneous Geological Media. Geofluids, **2018**, 1, **2018**.

27. KU C.Y., LIU C.Y., XIAO J.E., YEIH W., FAN C.M. A Spacetime Meshless Method for Modeling Subsurface Flow with a Transient Moving Boundary. Water, **11** (2595), 1, **2019**.

28. YANG L.X., SU Y., KU C.Y. Study on groundwater in coastal leakage aquifer system based on the Trefftz method. Journal of Fuzhou University (Natural Science Edition), **48** (6), 794, **2020** [In Chinese].

29. XI Q., FU Z.J., WU W.J., WANG H., WANG Y. A novel localized collocation solver based on Trefftz basis for potential-based inverse electromyography. Applied Mathematics and Computation, **390**, **2021**.

30. LIU C.S. A Fictitious Time Integration Method for Two-Dimensional Quasilinear Elliptic Boundary Value Problems. Computer Modeling in Engineering and Sciences, **33** (2), 179, **2008**.

31. KU C.Y., HONG L.D., LIU C.Y., XIAO J.E., HUANG W.P. Modeling Transient Flows in Heterogeneous Layered Porous Media Using the Space-Time Trefftz Method. Applied Sciences, **11** (8), 3421, **2021**.

32. JU L.X. Harbin subway survey pumping test and hydrogeological parameters calculation - take Line 3 V as an example. Master degree, Heilongjiang University, Heilongjiang, **2017** [In Chinese].